JACS
JOURNAL OF THE AMERICAN CHEMICAL SOCIETY
pubs.acs.org/JACS
Article

Synthesis, Isolation, and Study of Heterobimetallic Uranyl Crown Ether Complexes

Riddhi R. Golwankar,[#] Alexander C. Ervin,[#] Małgorzata Z. Makoś, Emily R. Mikeska, Vassiliki-Alexandra Glezakou,* and James D. Blakemore*

Cite This: https://doi.org/10.1021/jacs.3c12075
Read Online

ABSTRACT: Although crown ethers can selectively bind many metal cations, little is known regarding the solution properties of crown ether complexes of the uranyl dication, UO_2^{2+}. Here, the synthesis and characterization of isolable complexes in which the uranyl dication is bound in an 18-crown-6-like moiety are reported. A tailored macrocyclic ligand, templated with a Pt(II) center, captures UO_2^{2+} in the crown moiety, as demonstrated by results from single-crystal X-ray diffraction analysis. The U(V) oxidation state becomes accessible at a quite positive potential ($E_{1/2}$) of −0.18 V vs $Fc^{+/0}$ upon complexation, representing the most positive U^{VI}/U^{V} potential yet reported for the UO_2^{n+} core. Isolation and characterization of the U(V) form of the crown complex are also reported here; there are no prior reports of reduced uranyl crown ether complexes, but U(V) is clearly stabilized by crown chelation. Joint computational studies show that the electronic structure of the U(V) form results in significant weakening of U−O_{oxo} bonding despite the quite positive reduction potential at which this species can be accessed, underscoring that crown-ligated uranyl species could demonstrate unique reactivity under only modestly reducing conditions.

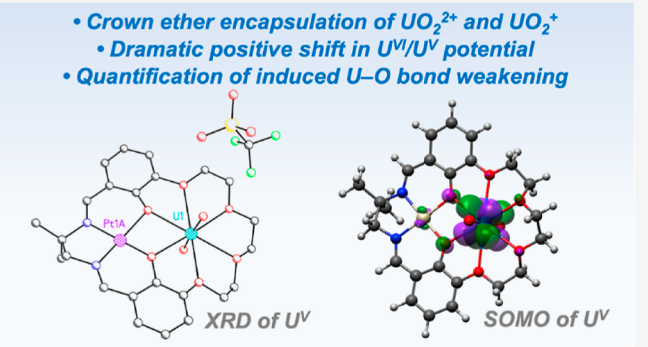

INTRODUCTION

The ability of crown ethers to chelate alkali-, alkaline-earth-, and transition-metal ions has been extensively documented through both crystallography and chemical analysis.[1] From the perspectives of both coordination chemistry and supramolecular science, the binding of metal cations in crown ether ligands has been demonstrated to impart unique and otherwise inaccessible properties to the resulting metal complexes, including modulated solubility, unique metal geometry, and modified speciation. In the area of radiochemistry,[2] crown ethers have been shown, in accord with the classic literature on the properties of crown ethers, to afford advantages in liquid−liquid extractions of products of fission.[3]

Conversely, few reports have described the binding/chelation of actinides in crown ethers, despite the ubiquity of these ligands and their usefulness for the preparation of metal complexes. Most recently, 18-crown-6 complexes of Cf(III) and Am(III) were reported,[4] complementing older work on complexes featuring U(III)[5] and Pu(III)[6] encapsulated in 18-crown-6 ligands. Studies have also demonstrated that the *trans*-dioxo actinyl-type species of U(VI),[7−10] Np(V),[11,12] and Pu(V)[13] can be chelated by 18-crown-6 derivatives in the solid state (see Chart 1). Virtually nothing is known, however, regarding the properties of crown-chelated uranyl complexes in solution, a situation attributable to the apparent propensity of

Chart 1. Literature Examples of Crown Ether Complexes of Actinyl Ions[7,9,11−13,18]

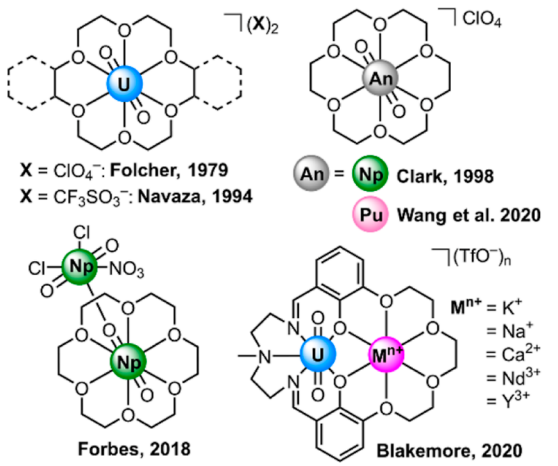

Received: October 29, 2023
Revised: February 18, 2024
Accepted: February 21, 2024

actinyl ions to be lost from simple 18-crown-6 derivatives in the presence of coordinating solvents such as water or dimethyl sulfoxide.[7,9,14] These findings have been thought to be in accord with the observation that the majority of related solid-state structures reveal actinide centers with water ligands in the first coordination sphere that hydrogen-bond to crown ethers held in the secondary sphere.[15] Additionally, although crown ethers and cryptands are ubiquitous in actinide organometallic chemistry, when they are utilized, they typically encapsulate countercations like Na^+ or K^+ that charge balance anionic actinide species.[16,17]

Considering the recognized usefulness of crown ethers as chelating ligands, and the observation that Ln(III) ions can undergo reduction to form less common Ln(II) analogues when ligated by crowns,[19] we anticipated that crown coordination of the uranyl ion has received less attention than it deserves. The reactivity and redox properties of crown-chelated actinyl ions are unknown to date, but we envisioned that accessing such species synthetically could enable study of uranyl reactivity in a formally neutral donor ligand set,[20] complementing much prior work that has examined charged ligands. We hypothesized that a dicationic complex of UO_2^{2+} could undergo electron transfer at a more modest potential than other derivatives with more negative overall charge states, favoring facile reduction. Overcoming the usual requirement of strong reductants for uranium could afford new insights applicable to next-generation nuclear fuel recycling systems involving uranium redox cycling.[21]

Here, we report that coordination of the uranyl ion by a macrocyclic crown ether ligand does indeed result in a dramatic positive shift of this species' U(VI)/U(V) reduction potential, likely a result of the dicationic nature of the crown UO_2^{2+} complex. On the basis of structural data from X-ray diffraction (XRD) analysis, it appears that tailored crown-ether-type ligands are uniquely well-suited for stabilizing the U(V) oxidation state. The accessibility of both U(VI) and U(V) crown complexes in solution could be favored in the system reported here by the installation of an accessory Pt(II)-containing site that enforces crown planarity and assists in uptake of uranyl. Computational studies with density functional theory (DFT) show that significant $U-O_{oxo}$ bond weakening is achieved upon generation of U(V) in this system, a finding in accord with prior work on this oxidation state but not previously accessible at such a modest reduction potential.

RESULTS AND DISCUSSION

In order to generate isolable uranyl-crown complexes, we developed a Pt(II)-templated macrocycle (denoted **1**) with a Reinhoudt-type ligand scaffold[22] that presents an 18-crown-6-like site for binding of the uranyl ion, UO_2^{2+}. In prior work, we have used crown-containing ligands to access lanthanide-binding Ni(II),[23] Pd(II),[24] Zn(II),[25] and V(IV)[26,27] complexes, but here, a new method was developed for installation of a platinum center into the macrocyclic framework with the goal of imparting stability and enabling future spectroscopic studies with ^{195}Pt NMR (see Experimental Section in Supporting Information for details). We found that **1** could be prepared from the previously reported [**H_2,Ba**][24] using $Ba(OH)_2{\cdot}8H_2O$ as a base and $Pt(DMSO)_2Cl_2$ as a metalating agent (Scheme 1). With our procedure, **1** could be isolated as an orange powder in good yield (ca. 70%) and fully characterized by ^{1}H and $^{13}C\{^1H\}$ NMR, UV−visible absorption spectroscopy, and elemental analysis (EA) (see Supporting Information, pp. S6, S9−S11, and S18).

Scheme 1. Synthetic Strategy for the Preparation of Complexes 1, 2, and 3[a]

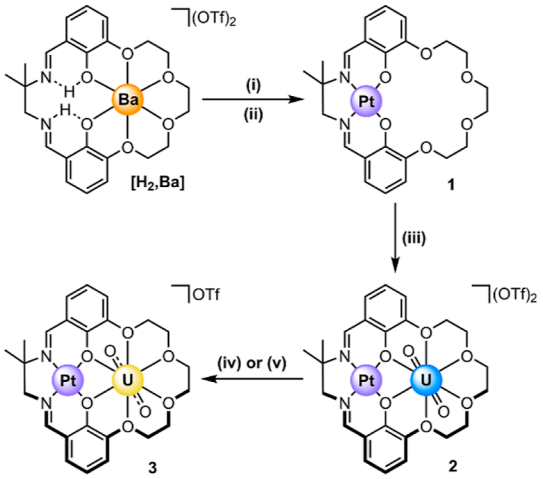

[a]Conditions: (i) 1.1 equiv $Ba(OH)_2{\cdot}8H_2O$, 0.95 equiv $PtCl_2(DMSO)_2$, in DMF and approx. 5 mL DMSO, 60−65 °C, 24 h; (ii) excess guanidinium sulfate in $CHCl_3$ and H_2O, 48 h. (iii) 1 equiv $UO_2(OTf)_2$ in CH_3CN, 30 min. (iv) 1 equiv Cp^*_2Fe in CH_3CN, 15 min; (v) 1 equiv Cp_2Co in CH_3CN, 15 min. The resulting $Cp^*_2Fe^+(OTf)^-$ [from route (iv)] or $Cp_2Co^+(OTf)^-$ [from route (v)] can be washed away to yield pure **3**.

Single crystals of **1** suitable for XRD analysis were grown by the vapor diffusion of hexanes into a dichloromethane (CH_2Cl_2) solution of the complex. In line with NMR spectral findings, the XRD structure of **1** (Figure 1) confirmed the binding of Pt(II) in the salen-like [N_2,O_2] site of the ligand; a single co-crystallized water molecule was found interacting with the crown-ether-like site via H-bonding in the solid state, but we note that the complex can be fully dried, resulting in removal of water without any decomposition. Importantly, the platinum site is rigorously square planar (τ_4 = 0.04(1)) and thus appears to assist in enforcing a high degree of flatness across the full macrocyclic structure. The planarity of the crown-ether-like site was quantified through the ω_{crown} parameter (*vide infra*); the value of this parameter for **1** is 0.20(1), in accord with prearrangement of the six oxygen donors of the crown site and their readiness to bind UO_2^{2+} (see Table 1). Details for all the structures from XRD analysis are given in the Supporting Information on pp. S37−S59.

UO_2^{2+} was installed into the crown site by addition of 1 equiv of anhydrous uranyl triflate, $UO_2(OTf)_2$, to **1** in CH_3CN. $UO_2(OTf)_2$ was prepared according to Ephritikhine's method,[28] with minor modifications as described in a prior report from our group.[29] Addition of anhydrous $UO_2(OTf)_2$ to **1** resulted in an immediate change in the color of the solution from mango yellow to deep red; the resulting heterobimetallic uranyl crown complex (denoted as **2**) could be isolated in virtually quantitative yield by filtration followed by removal of solvent in vacuo. ^{1}H, $^{13}C\{^1H\}$, and $^{19}F\{^1H\}$ NMR spectra collected in CD_3CN (see Supporting Information, pp. S12−S15) confirmed the formation of **2** and its persistence in solution; a characteristic and significant downfield shift of the ^{1}H NMR resonances associated with the aliphatic protons of the ethylene bridges of the crown was measured (from 3.6−4.1 ppm to 5.2−5.5 ppm) in line with threading of the uranyl ion

https://doi.org/10.1021/jacs.3c12075
J. Am. Chem. Soc. XXXX, XXX, XXX−XXX

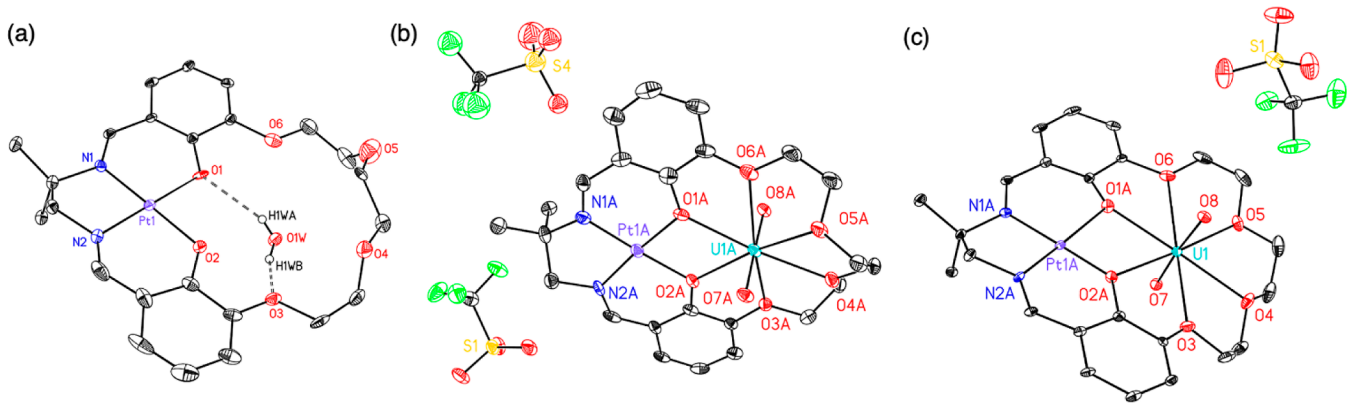

Figure 1. Solid-state structures (XRD) of (a) **1**, (b) **2**, and (c) **3**. Two nearby triflate counteranions from the asymmetric unit are shown for **2**. All hydrogen atoms except for those associated with the cocrystallized water molecule in **1**, co-crystallized CH_3CN molecules, and minor components of disorder are omitted for clarity. Displacement ellipsoids are shown at the 20% probability level.

Table 1. Comparison of Selected Structural Parameters for 1, 2, and 3 from XRD Analysis

	1	2	3
U−O_{oxo} (Å)[a]		1.751(9)[f]	1.819(4)
U−O_{phen} (Å)[a]		2.41(1)[f]	2.53(3)[e]
Pt−O_{phen} (Å)[a]	2.00(4)[e]	1.99(2)[f]	2.01(2)[e]
C−N_{imine} (Å)[a]	1.39(3)[e]	1.29(3)[f]	1.29(2)[e]
O1···O2	2.74(5)[e]	2.59(2)[f]	2.64(4)[e]
Pt···U (Å)		3.535(1)[f]	3.655(1)[e]
τ_4[b]	0.04(1)[e]	0.05(2)[f]	0.07(3)[e]
ω_{crown} (Å)[c]	0.20(1)[e]	0.23(3)[f]	0.12(2)[e]
Ψ_U (Å)[d]		0.05(1)	0.03(1)

[a]Defined as the average of the interatomic distances between the noted atom types. [b]Geometry index for four-coordinate complexes, with the values ranging from 1.00 to 0.00 for perfectly tetrahedral and square-planar geometries, respectively; see ref 31 for details. [c]Defined as root-mean-square deviation (rmsd) of O1−O6. [d]Defined as the absolute value of the distance between the uranium atom and the mean plane defined by O1−O6. [e]Values are reported as the mean of the relevant individual values corresponding to two disordered molecular orientations occupying the same site in the asymmetric unit. [f]Values were calculated as the mean of the relevant individual values corresponding to two independent molecules occupying distinct sites in the asymmetric unit. Stated e.s.ds. on averaged distances were taken as the largest of the individual values in the refined data for the independent molecular species. Stated e.s.ds. on the τ_4, ω_{crown}, and Ψ_U values were calculated as the standard deviation of the set of relevant values from the structural data. See Table S3 for details.

into the crown. However, in line with the dicationic and highly Lewis acidic nature of UO_2^{2+}, downfield shifts were observed for all of the other ^1H resonances associated with the ligand backbone of **2** in comparison to those for **1** (Figure S19).

Chelation of UO_2^{2+} by the crown ether oxygen atoms in **2** was confirmed by the single-crystal XRD structure (Figure 1) of the heterobimetallic complex. Single crystals of **2** suitable for XRD analysis were grown by the vapor diffusion of Et_2O into a CH_3CN solution of the complex. As anticipated from the NMR studies, the uranyl dication was found in the crown-ether-like site of the macrocyclic ligand, interacting with all six macrocyclic oxygen donor atoms. No additional solvent molecules or triflate counteranions bind to the U center; the triflate counteranions (2 per $[UO_2]$ unit) were found in the outer sphere along with co-crystallized CH_3CN molecules presumably derived from the crystal growth conditions. The average U−O_{oxo} bond distance was found to be 1.751(9) Å (Table 1), in line with the U(VI) formal oxidation state[30] and the dicationic nature of the overall $[Pt,UO_2]^{2+}$ species.

In line with findings from prior work on crown systems from our group that examined binding of other cations, UO_2^{2+} nestles most closely toward the phenoxide O atoms that bridge to the Pt(II) center (Figure S66) and sits most far away from O3/O6 in the crown-like site. The binding of UO_2^{2+} results in an overall contraction of the average O1···O2 distance of the nascent heterobimetallic diamond core motif, from 2.74(5) Å in **1** to 2.59(2) Å in **2**; this is consistent with the Lewis acidic nature of UO_2^{2+} and interaction of both Pt^{2+} and UO_2^{2+} with the bridging atoms.

Further examination of the structures from XRD reveals a possible basis for the stability of **2** in solution. In our work with crown complexes, we have used a parameter denoted ω_{crown} to quantify the degree of planarity of the O atoms in the crown-like sites of our macrocycles.[23] ω_{crown} is defined as the rmsd of the O atoms of the crown moiety from the mean plane defined by their positions. Thus, lower values of ω_{crown} correspond to more planar sites for metal chelation. The average ω_{crown} parameter for **2** is 0.23(3), similar to the value of 0.20(1) found for **1**, suggesting that little reorganization of the ligand is required for uranyl binding. Additionally, the ω_{crown} values of a representative set of structures of bare 18-crown-6 ligands lacking interactions with ions[32] are all larger (spanning from 0.228 to 0.254) than the value for **1** of 0.20(1), suggesting that the accessory Pt(II)-containing site enhances the net planarity of the crown, poising it for uranyl capture. In accord with this theory, the out-of-plane deviations of the nascent bridging phenoxide O atoms are significantly smaller in **1** (0.121 for O1 and 0.216 for O2) than the O-atoms of the bare crowns (spanning from 0.228 to 0.254). The rigorous square-planar coordination geometry of the Pt(II) center thus appears to assist in bringing the crown into a conformation ideal for uranyl binding.

With **2** in hand, we moved to interrogate the redox properties of the complex in light of its unusual structure and the formally dicationic nature of the heterobimetallic $[Pt,UO_2]$ core, which we anticipated could lead to uncommon properties. As a preamble, we note that the electrochemical properties of the precursor **1** are unremarkable; cyclic voltammetry (CV) data show that this complex features a single reduction event, likely ligand-centered in nature,[24,25]

https://doi.org/10.1021/jacs.3c12075
J. Am. Chem. Soc. XXXX, XXX, XXX−XXX

with a peak cathodic reduction potential ($E_{p,c}$) of −2.44 V vs ferrocenium/ferrocene (denoted hereafter as $Fc^{+/0}$) in CH_3CN containing 0.1 M tetrabutylammonium hexafluorophosphate ($TBAPF_6$) (Figures S42 and S43).

Contrasting with the profile measured for **1**, CV data for **2** exhibit a unique quasi-reversible redox process with $E_{1/2}$ = −0.18 V vs $Fc^{+/0}$ (Figures 2a and S44). Scan-rate-dependent

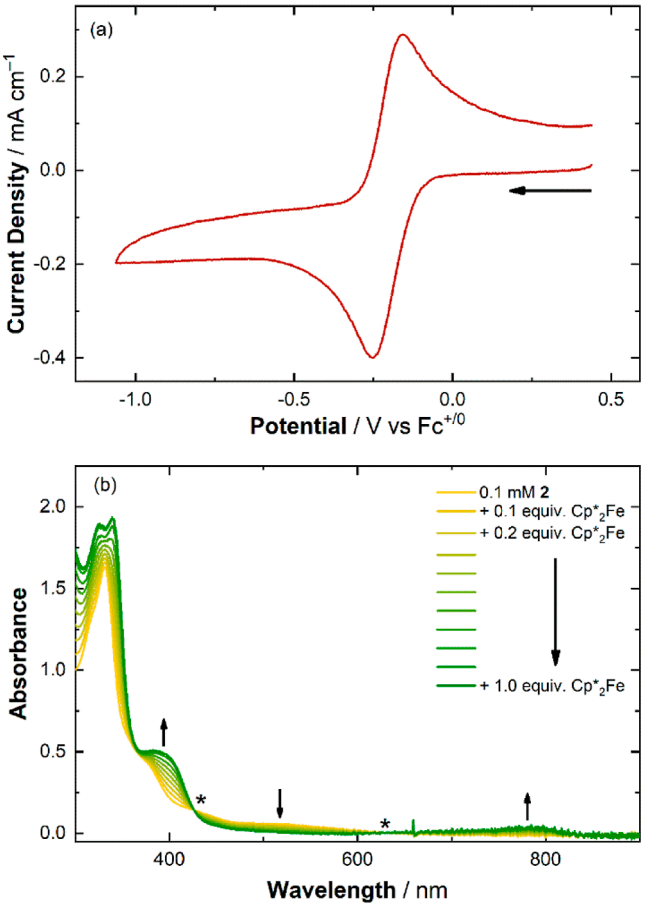

Figure 2. Panel (a): cyclic voltammogram of **2** in CH_3CN (0.1 M $[^nBu_4N]^+[PF_6]^-$, 100 mV/s) showing the U^{VI}/U^V redox couple. Panel (b): spectrochemical titration data for **2** with 1 equiv of Cp^*_2Fe in CH_3CN. Isosbestic points are denoted by asterisks (*) and located at 426 and 630 nm.

data (50−300 mV/s; see Figure S45) confirmed the freely diffusional behavior of both the oxidized and reduced forms of the complex at the electrode, and we note that the peak-to-peak separation of the anodic and cathodic processes (ΔE_p) was 98 mV at 100 mV/s scan rate, indicative of rapid electron transfer behavior and fast interconversion of the oxidized and reduced forms of **2** at the electrode surface.[33] As the ratio of the anodic to cathodic peak currents is near unity for all scan rates that we tested, we conclude that the reduction of **2** is chemically reversible (Figure S46). As CV data for the blank electrolyte and **1** lack any features resembling the wave measured for **2** at −0.18 V (Figure S47), this wave could be assigned as being $1e^-$ in nature and corresponding to generation of a complex, denoted **3**, that features uranium in the +5 oxidation state (for further characterization, *vide infra*). To the best of our knowledge, this redox chemistry represents the most positive reduction potential yet measured for U^{VI}/U^V redox cycling in a uranyl ion in which the oxo ligands (terminal O^{2-} groups) are not bonded to other chemical species, metal ions, or Lewis acids.[34] On the basis of comparison to literature complexes, the U(VI)/U(V) reduction potential in the crown for **2** is shifted by ca. + 1.3 V relative to model neutral complexes of the uranyl ion, underscoring the dramatic effect induced by crown chelation.[18,30,34] This dramatic shift in the U^{VI}/U^V couple that favors reduction can be attributed to the dicationic nature of the U(VI) complex and particular stabilization of the U(V) oxidation state by crown ether chelation.

In order to understand these electrochemical findings and to validate the $1e^-$ nature of the reduction process at −0.18 V, we conducted chemical reduction experiments. We have found that decamethylferrocene (Cp^*_2Fe), a mild, outer-sphere electron-transfer agent with $E_{1/2}$ = −0.48 V,[35] is sufficiently reducing to drive conversion of U(VI) to U(V), as demonstrated by titration of **2** with Cp^*_2Fe (Figure 2b). The electronic spectrum of **2** in CH_3CN (0.1 mM) displays prominent features with $\lambda_{max} \approx$ 232, 259, and 331 nm, along with weaker absorbing features with $\lambda_{max} \approx$ 376 and 513 nm (Figures S22 and S23). However, upon addition of 1 equiv of Cp^*_2Fe, the spectral profile changes dramatically and isosbestically with U(V) and Fe(III) generation. The spectra confirm that conversion to the products is clean and complete, with isosbestic points at 426 and 630 nm; additionally, a feature at 784 nm can be confidently assigned as arising from a d−d transition associated with coproduced $Cp^*_2Fe^+$ (Figures S24 and S26). Additions of Cp^*_2Fe beyond 1 equiv led to no further significant spectral changes (Figures S25 and S29), in line with the CV data and the potentials accessible to Fe(II)-driven reduction. In accord with the measured $E_{1/2}(U^{VI}/U^V)$ of −0.18 V, we found that cobaltocene (Cp_2Co) is also capable of generating **3** (Figures S27 and S28), consistent with its more negative $E_{1/2}$ value under our conditions of −1.33 V (Figures S48 and S49).

To build up evidence that the observed reduction was uranium-centered, we collected near-infrared (NIR) spectra on *in situ*-generated **3** (Figures 3 and S31−S35). U(V) centers have been shown to exhibit sharp transitions in the NIR region with modest extinction coefficients (ε values) of ca. 10^2 M^{-1} cm^{-1}, providing a spectral signature for this oxidation state.[36] **2** does not exhibit transitions in the NIR region, in line with the U(VI) oxidation state, but reduction of this complex by 1 equiv of either Cp^*_2Fe or Cp_2Co results in the appearance of two sharp features with λ_{max} = 1375 and 1410 nm (7272 and 7090 cm^{-1}) and ε values of 8.7 and 8.0 M^{-1} cm^{-1}, respectively. These modest values are consistent with Laporte-forbidden 5f-to-5f transitions and resemble examples in the literature,[36] providing support for the generation of U(V).

Solution-state Raman spectroscopy was also conducted on **2** and *in situ*-generated **3**. The Raman spectrum of **2** reveals the presence of the uranyl moiety, with a distinctive feature corresponding to the symmetric stretch (ν_{sym}) at 874 cm^{-1} (Figure S41).[30] Upon reduction to form **3**, this feature was lost, in accord with complete reduction of uranium. The spectra of **3** were checked for observation of ν_{sym} at lower wavenumbers, but no features could be reliably attributed to U(V); the relevant spectral region from 870 to 700 cm^{-1}, however, displays a large feature associated with solvent that could mask signal(s) associated with reduced uranyl.

Encouraged by the spectroscopic results, we attempted chemical preparation and isolation of the $1e^-$ reduced complex **3** in CH_3CN. In order to achieve this, **2** was treated with 1

https://doi.org/10.1021/jacs.3c12075
J. Am. Chem. Soc. XXXX, XXX, XXX−XXX

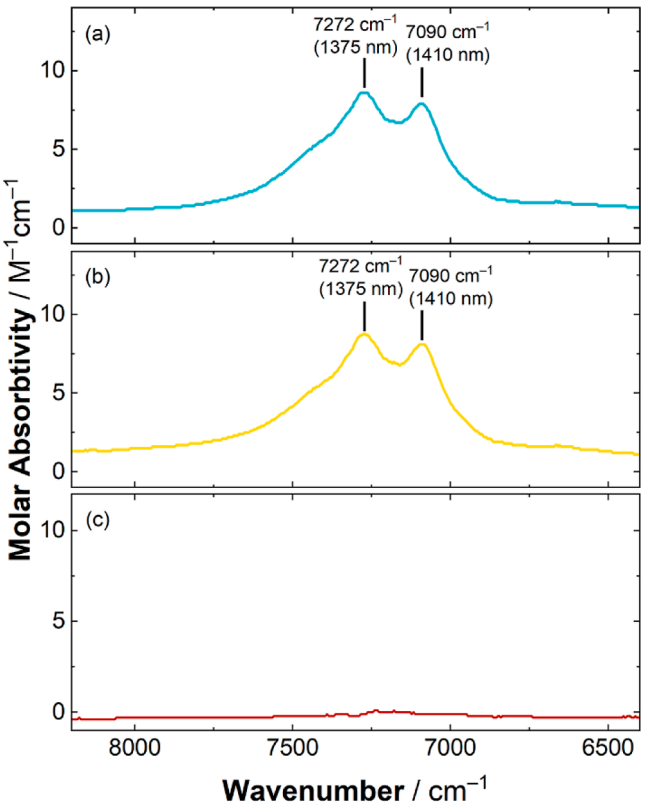

Figure 3. NIR spectra. Spectrum a (blue line): **3** generated by in situ reduction with Cp^*_2Fe. Spectrum b (yellow line): **3** generated by *in situ* reduction with Cp_2Co. Spectrum c (red line): **2** dissolved in CH_3CN. Conditions: [U] = 10 mM in CH_3CN.

equiv of Cp^*_2Fe in CH_3CN, resulting in an immediate color change of the solution from dark red to green. The solvent was removed *in vacuo* to obtain a green powder which was found to contain a 1:1 mixture of **3** and $Cp^*_2Fe(OTf)$ (mixture denoted as **3a**). A similar procedure using Cp_2Co as a reductant yielded a yellow-orange powder containing a 1:1 mixture of **3** and $Cp_2Co(OTf)$ (mixture denoted as **3b**). In line with the similar solubilities of **3** and the metallocenium triflate salts, we found **3** challenging to isolate alone; the mixtures denoted **3a** and **3b** can be used for characterization or **3** can be separated and obtained in pure form by washing of **3b** with 1,2-dichloroethane. The ^1H NMR spectra of **3a** and **3b** (d_3-CH_3CN) (Figures S17 and S18) confirm the formation of $Cp^*_2Fe^+$ and Cp_2Co^+, respectively; 10 new paramagnetically shifted resonances common to the spectra of **3**, **3a**, and **3b** were observed as well, consistent with clean, stoichiometric reduction of **2**. EA confirmed the formulations of **3**, **3a**, and **3b** (see Supporting Information, p. S7), suggesting that the U(V) species is stable under an inert atmosphere; this is in accord with its relatively positive reduction potential, which could engender stability during transport to the EA facility.

Crystals of **3** suitable for XRD analysis were grown by diffusion of Et_2O into a concentrated propionitrile solution containing the complex. In the structure that was obtained, the identities of the ligands in the first coordination sphere of uranium are identical to those found in the U(VI) analogue **2**, in accord with transfer of $1e^-$ to form **3** but with no further chemical reactivity. The average $U-O_{oxo}$ bond distance is elongated to 1.819(4) Å; this elongation by 0.068 Å is consistent with U-centered reduction and formation of the U(V) oxidation state,[30] in line with the findings from NIR spectroscopy (Figure 3). The $U-O_{phenoxide}$ distances are elongated in **3**, consistent with generation of a more electron-rich uranium center upon reduction and attenuation of the effective Lewis acidity of the U center in this oxidation state (Table 1). The $C-N_{imine}$ distances in **2** and **3** are indistinguishable, however, supporting localization of the added electron density on uranium and little participation of the Pt site in the reduction process. The ω_{crown} parameter value of 0.12(2) in **3** is decreased from the value of 0.23(3) in **2**, suggesting that the less Lewis acidic U(V) oxidation state diminishes the out-of-plane distortion of the crown-ether-like site; this finding is in accord with our prior studies of Lewis-acidity-dependent crown behaviors in related Pd and Ni complexes.[23,24] On the basis of the Ψ_U values for **2** and **3**, U(V) can be concluded to sit more closely in the plane of the oxygen donor ligands than U(VI), suggesting an attractive supramolecular fit of $[U^VO_2]^+$ in the crown site.

DFT calculations were performed to probe the electronic structure of the crown-ligated uranium complexes prepared in this study and to understand the measured weakening of the $U-O_{oxo}$ interactions upon formation of the U(V) oxidation state. Starting with the coordinates of the structure of **2** from XRD, geometry optimizations were executed for the U(VI) complex with an overall charge of +2 (**2**) and the U(V) complex with an overall charge of +1 (**3**) at the PBE0/ZORA-def2-TZVP (H, C, N, O)/SARC-ZORA-TZVP (Pt, U)[37,38] (Table S1) level of theory. The structures were optimized both in the gas phase and using polarizable continuum solvation[39] for acetonitrile. Both calculations showed similar results, as can be seen in Table S1. The computed geometry parameters closely align with XRD data, demonstrating minimal differences within ±1.7% of the corresponding experimental values, showing a high degree of agreement. Additionally, a comparison of five different basis sets showed only small variations (Tables S2−S4). Based on the calculations in the gas phase, the asymmetric $U-O_{oxo}$ stretching vibration of **2** was predicted to decrease by 114 cm^{-1} upon reduction, consistent with significant bond weakening. Experimental spectra were collected for both **2** and **3** in the solid state, and the relevant vibrations were found to shift by 137 cm^{-1} (see Supporting Information, pp. S26−S28, S34, and S35), confirming that there is a significant weakening of the $U-O_{oxo}$ bonding upon reduction despite the rather positive potential measured for U(V) generation in this system.

The calculations carried out for U(VI) species **2** reveal a distinctly metal-centered LUMO bearing strong resemblance to the $f_{y^3-3yx^2}$ orbital, suggesting that the site of reduction in this complex would be centered primarily on uranium (Figure 4). In line with this thesis, the SOMO of **3** is largely centered on uranium, although this orbital bears a strong resemblance to an $f_{zx^2-zy^2}$ orbital, suggesting shifted occupation of a different 5f orbital upon relaxation of the complex following reduction. The LUMO of **3**, however, is predominantly delocalized over the conjugated ligand backbone, in line with the experimental observation of a further irreversible reduction at −2.04 V for this species (Figure S44).

NBO charge analysis[40−42] reveals a charge of +1.855|*e*| at the U center in **2**; the charge at U decreases to +1.591|*e*| in **3**, in line with the generation of the U(V) formal oxidation state in this species (Table S2). Furthermore, charge analysis indicates that there is buildup of negative charge on each of the oxo moieties (*yl* oxygens) by ca. −0.2|*e*| per oxo upon U-centered

https://doi.org/10.1021/jacs.3c12075
J. Am. Chem. Soc. XXXX, XXX, XXX−XXX

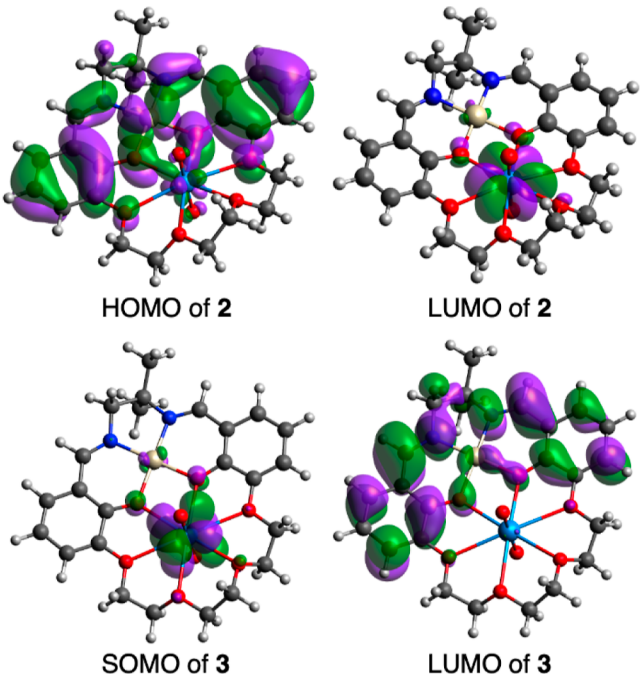

Figure 4. HOMO and LUMO of **2** (upper structures) and SOMO and LUMO of **3** (lower structures). The localization of the LUMO of **2** and the SOMO of **3** on the uranium metal center is consistent with the generation of uranium(V) in **3**.

reduction. This finding suggests that the *yl* moieties in **3** are more basic than in **2**[30] and could be more susceptible to reactivity with acidic reagents, a prospect currently under investigation.

CONCLUSIONS

In conclusion, heterobimetallic complexes in which the uranyl ion is captured and coordinated in a crown ether coordination environment have been synthesized and fully characterized. The findings reported here suggest that crown-ether-type ligands could be quite useful for the generation of uranium complexes with unique properties, including rather positive reduction potentials and modulated reactivity, in comparison to more conventional complexes. The formation of a U(VI) complex with a +2 overall charge and a U(V) complex with a +1 overall charge in this work appears to promote these unusual features. We note that well-characterized uranyl crown complexes are rare, but the macrocyclic crown ether featuring an accessory Pt(II) center presented here can chelate both U(VI) and U(V) in solution and disfavors binding of exogeneous, anionic triflate ligands to the uranium center, despite the conventional propensity of uranyl to bind anionic ligands when possible. Both the U(VI) and U(V) forms of the uranyl ion can be stably chelated by the crown ether, opening a significant new synthetic space to explore tuning of uranium-centered chemistry through systematic crown-ligand modification. Thorough experimental and theoretical exploration of the properties of uranyl crown complexes is now in progress in our laboratories.

ASSOCIATED CONTENT

Supporting Information

The Supporting Information is available free of charge at https://pubs.acs.org/doi/10.1021/jacs.3c12075.

Spectroscopic, electrochemical, and structural data; information on computational methods; and DFT-optimized Cartesian coordinates and computed energies (PDF)

Cartesian coordinates for experimental XRD structures (XYZ)

Cartesian coordinates for DFT-optimized structures (XYZ)

Accession Codes

CCDC 2295456−2295458 contain the supplementary crystallographic data for this paper. These data can be obtained free of charge via www.ccdc.cam.ac.uk/data_request/cif or by emailing data_request@ccdc.cam.ac.uk or by contacting The Cambridge Crystallographic Data Centre, 12 Union Road, Cambridge CB2 1EZ, UK; fax: +44 1223 336033.

AUTHOR INFORMATION

Corresponding Authors

Vassiliki-Alexandra Glezakou − *Chemical Sciences Division, Oak Ridge National Laboratory, Oak Ridge, Tennessee 37830, United States;* orcid.org/0000-0001-6028-7021; Email: glezakouva@ornl.gov

James D. Blakemore − *Department of Chemistry, University of Kansas, Lawrence, Kansas 66045, United States;* orcid.org/0000-0003-4172-7460; Email: blakemore@ku.edu

Authors

Riddhi R. Golwankar − *Department of Chemistry, University of Kansas, Lawrence, Kansas 66045, United States;* orcid.org/0000-0003-3957-7862

Alexander C. Ervin − *Department of Chemistry, University of Kansas, Lawrence, Kansas 66045, United States*

Małgorzata Z. Makoś − *Chemical Sciences Division, Oak Ridge National Laboratory, Oak Ridge, Tennessee 37830, United States*

Emily R. Mikeska − *Department of Chemistry, University of Kansas, Lawrence, Kansas 66045, United States;* orcid.org/0000-0001-5149-0132

Complete contact information is available at: https://pubs.acs.org/10.1021/jacs.3c12075

Author Contributions

#R.R.G. and A.C.E. contributed equally to this work. The manuscript was written through contributions of all authors. All authors have given approval to the final version of the manuscript.

Notes

The authors declare no competing financial interest.

ACKNOWLEDGMENTS

Dedicated to Prof. Victor W. Day on the occasion of his 80th birthday. This work was supported by the U.S. Department of Energy, Office of Science, Office of Basic Energy Sciences through the Early Career Research Program (DE-SC0019169). A.C.E. was supported by a U.S. National Science Foundation Research Traineeship (NRT) at the University of Kansas (DGE-1922649). M.Z.M. and V.A.G. were supported by ORNL's Laboratory Directed Research and Development (LDRD) program. This research used resources of the National Energy Research Scientific Computing Center (NERSC), a U.S. Department of Energy Office of Science

User Facility located at Lawrence Berkeley National Laboratory, operated under contract no. DE-AC02-05CH11231. Analytical data were obtained from the CENTC Elemental Analysis Facility at the University of Rochester, supported by the US National Science Foundation through award CHE-0650456. The authors thank Michael K. Takase (Beckman Institute, Caltech) for assistance with refinement of the structure of **2** obtained by single-crystal XRD analysis.

REFERENCES

(1) (a) Pedersen, C. J. Cyclic polyethers and their complexes with metal salts. *J. Am. Chem. Soc.* **1967**, *89*, 7017−7036. (b) Truter, M. R. Structures of organic complexes with alkali metal ions. In *Alkali Metal Complexes with Organic Ligands*; Springer, 2005, pp 71−111. (c) Farago, M. Transition metal complexes of "crown" ethers. *Inorg. Chim. Acta* **1977**, *25*, 71−76. (d) Steed, J. W. First-and second-sphere coordination chemistry of alkali metal crown ether complexes. *Coord. Chem. Rev.* **2001**, *215*, 171−221.

(2) Nesterov, S. V. Crown ethers in radiochemistry. Advances and prospects. *Russ. Chem. Rev.* **2000**, *69*, 769−782.

(3) (a) Jalhoom, M. G.; Mani, I. A.; Juburi, J. A. A. Radiochemical separations by use of crown ethers and cryptates. *Radiochim. Acta* **1985**, *38*, 215−218. (b) Shukla, J.; Singh, R.; Kumar, A. Extraction of uranium (VI) and plutonium (IV) into toluene by crown ethers from nitric acid solution. *Radiochim. Acta* **1991**, *54*, 73−78. (c) Billard, I.; Ouadi, A.; Gaillard, C. Liquid−liquid extraction of actinides, lanthanides, and fission products by use of ionic liquids: from discovery to understanding. *Anal. Bioanal. Chem.* **2011**, *400*, 1555−1566.

(4) Poe, T. N.; Ramanantoanina, H.; Sperling, J. M.; Wineinger, H. B.; Rotermund, B. M.; Brannon, J.; Bai, Z.; Scheibe, B.; Beck, N.; Long, B. N.; Justiniano, S.; Albrecht-Schönzart, T. E.; Celis-Barros, C. Isolation of a californium (II) crown−ether complex. *Nat. Chem.* **2023**, *15*, 722−728.

(5) (a) Dejean, A.; Charpin, P.; Folcher, G.; Rigny, P.; Navaza, A.; Tsoucaris, G. Insertion of trivalent uranium in macrocyclic crown-ethers: EXAFS and X-ray structural analyses. *Polyhedron* **1987**, *6*, 189−195. (b) Arliguie, T.; Belkhiri, L.; Bouaoud, S.-E.; Thuéry, P.; Villiers, C.; Boucekkine, A.; Ephritikhine, M. Lanthanide (III) and actinide (III) complexes $[M(BH_4)_2(THF)_5]$ $[BPh_4]$ and $[M(BH_4)_2(18\text{-crown-}6)]$ $[BPh_4]$ (M= Nd, Ce, U): synthesis, crystal Structure, and density functional theory investigation of the covalent contribution to metal-borohydride bonding. *Inorg. Chem.* **2009**, *48*, 221−230.

(6) Li, K.; Hu, S.; Zou, Q.; Zhang, Y.; Zhang, H.; Zhao, Y.; Zhou, T.; Chai, Z.; Wang, Y. Synthesis and characterizations of a plutonium (III) crown ether inclusion complex. *Inorg. Chem.* **2021**, *60*, 8984−8989.

(7) Folcher, G.; Charpin, P.; Costes, R.-M.; Keller, N.; Villardi, G. C. . d. Anhydrous uranyl crown-ether complexes. ^{1}H nuclear magnetic resonance and x-ray study. *Inorg. Chim. Acta* **1979**, *34*, 87−90.

(8) Navaza, A.; Villain, F.; Charpin, P. Crystal structures of the dicyclohexyl-(18-crown-6) uranyl perchlorate complex and of its hydrolysis product. *Polyhedron* **1984**, *3*, 143−149.

(9) Deshayes, L.; Keller, N.; Lance, M.; Navaza, A.; Nierlich, M.; Vigner, J. EXAFS analysis of aqueous and acetonitrile solutions of UO_2-trilate with crown-ethers and aza-crowns. Crystals structures of the inclusion complexes $UO_2(18\text{-crown-}6)(CF_3SO_3)_2$ and $UO_2(\text{dicyclohexyl-}18\text{-crown-}6)(CF_3SO_3)_2$. *Polyhedron* **1994**, *13*, 1725−1733.

(10) Nierlich, M.; Sabattie, J.-M.; Keller, N.; Lance, M.; Vigner, J.-D. Inclusion complex between uranyl and an azacrown; structure of $[UO_2(18\text{-azacrown-}6)]^{2+}\bullet\ 2CF_3SO_3^-$. *Acta Crystallogr., Sect. C: Cryst. Struct. Commun.* **1994**, *50*, 52−54.

(11) Clark, D. L.; Keogh, D. W.; Palmer, P. D.; Scott, B. L.; Tait, C. D. Synthesis and Structure of the First Transuranium Crown Ether Inclusion Complex: $[NpO_2$ ([18]Crown-6)$]$ ClO_4. *Angew. Chem., Int. Ed.* **1998**, *37*, 164−166.

(12) Basile, M.; Cole, E.; Forbes, T. Z. Impacts of oxo interactions on Np(V) crown ether complexes. *Inorg. Chem.* **2018**, *57*, 6016−6028.

(13) Wang, Y.; Hu, S.-X.; Cheng, L.; Liang, C.; Yin, X.; Zhang, H.; Li, A.; Sheng, D.; Diwu, J.; Wang, X.; et al. Stabilization of Plutonium(V) Within a Crown Ether Inclusion Complex. *CCS Chem.* **2020**, *2*, 425−431.

(14) (a) There is one literature report (given in ref 14b) purporting to concern the single-crystal XRD structure of a complex in which the uranyl ion is chelated by 12-crown-4. However, the supposed structure is unrealistic, as it features U-to-O distances and macrocycle contacts with neighboring atoms that are too short. These observations suggesting that the structure is incorrect are in line with the assumption that a 12-crown-4 macrocycle should be too small to encapsulate UO_2^{2+}. The structure in question was obtained with film-recorded data in 1977, and the data workup included an absorption correction. However, Cu radiation was used; Mo radiation would have been better because of lower absorption and data could have been collected to high resolution. Considering the undoubtedly misplaced nitrate N atom, it could be that the true structure has U bound to nitrate rather than chelated by 12-crown-4 as proposed. (b) Armağan, N. 1, 4, 7, 10-Tetraoxacyclododecane-uranyl nitrate dihydrate. *Acta Crystallogr., Sect. B: Struct. Crystallogr. Cryst. Chem.* **1977**, *33*, 2281−2284.

(15) (a) Eller, P.; Penneman, R. Synthesis and structure of the 1:1 uranyl nitrate tetrahydrate-18-crown-6 compound, $UO_2(NO_3)_2(H_2O)_2\bullet 2H_2O\bullet$(18-crown-6). Noncoordination of uranyl by the crown ether. *Inorg. Chem.* **1976**, *15*, 2439−2442. (b) Rogers, R. D.; Kurihara, L. K.; Benning, M. M. f-Element/crown ether complexes, 11. Preparation and structural characterization of $[UO_2(OH_2)_5]$ $[ClO_4]_2\cdot 3(15\text{-crown-}5)\cdot CH_3CN$ and $[UO_2(OH_2)_5]$ $[ClO_4]_2\cdot 2(18\text{-crown-}6)\cdot 2\ CH_3CN\cdot H_2O$. *J. Inclusion Phenom.* **1987**, *5*, 645−658. (c) Deshayes, L.; Keller, N.; Lance, M.; Nierlich, M.; Vigner, D. Complexes between uranyl nitrate and benzo-15-crown-5: structures of the (2/1) and (1/1) complexes of benzo-15-crown-5−diaquadinitratodioxouranium(VI). *Acta Crystallogr., Sect. C: Cryst. Struct. Commun.* **1993**, *49*, 16−19. (d) Deshayes, L.; Keller, N.; Lance, M.; Nierlich, M.; Vigner, J.-D. Pentaaquadioxouranium(VI) triflate−18-crown-6. *Acta Crystallogr., Sect. C: Cryst. Struct. Commun.* **1994**, *50*, 1541−1544.

(16) (a) Pyrch, M. M.; Williams, J. M.; Forbes, T. Z. Exploring crown-ether functionalization on the stabilization of hexavalent neptunium. *Chem. Commun.* **2019**, *55*, 9319−9322. (b) MacDonald, M. R.; Ziller, J. W.; Evans, W. J. Synthesis of a crystalline molecular complex of Y^{2+}, [(18-crown-6) K] $[(C_5H_4SiMe_3)_3Y]$. *J. Am. Chem. Soc.* **2011**, *133*, 15914−15917.

(17) Keener, M.; Shivaraam, R. A. K.; Rajeshkumar, T.; Tricoire, M.; Scopelliti, R.; Zivkovic, I.; Chauvin, A.-S.; Maron, L.; Mazzanti, M. Multielectron Redox Chemistry of Uranium by Accessing the + II Oxidation State and Enabling Reduction to a U(I) Synthon. *J. Am. Chem. Soc.* **2023**, *145*, 16271−16283.

(18) Kumar, A.; Lionetti, D.; Day, V. W.; Blakemore, J. D. Redox-Inactive Metal Cations Modulate the Reduction Potential of the Uranyl Ion in Macrocyclic Complexes. *J. Am. Chem. Soc.* **2020**, *142*, 3032−3041.

(19) (a) Ryan, A. J.; Ziller, J. W.; Evans, W. J. The importance of the counter-cation in reductive rare-earth metal chemistry: 18-crown-6 instead of 2,2,2-cryptand allows isolation of $[Y^{II}(NR_2)_3]^{1-}$ and ynediolate and enediolate complexes from CO reactions. *Chem. Sci.* **2020**, *11*, 2006−2014. (b) Huh, D. N.; Ziller, J. W.; Evans, W. J. Isolation of reactive Ln(II) complexes with C_5H_4Me ligands (Cp^{Me}) using inverse sandwich countercations: synthesis and structure of $[(18\text{-crown-}6)K(\mu\text{-}Cp^{Me})K(18\text{-crown-}6)]$ $[Cp^{Me}{}_3Ln^{II}]$ (Ln= Tb, Ho). *Dalton Trans.* **2018**, *47*, 17285−17290. (c) Xemard, M.; Cordier, M.; Molton, F.; Duboc, C.; Le Guennic, B.; Maury, O.; Cador, O.; Nocton, G. Divalent thulium crown ether complexes with field-induced slow magnetic relaxation. *Inorg. Chem.* **2019**, *58*, 2872−2880.

https://doi.org/10.1021/jacs.3c12075
J. Am. Chem. Soc. XXXX, XXX, XXX−XXX

(20) (a) Dalley, N. K.; Mueller, M. H.; Simonsen, S. H. Neutron diffraction study of monoaquotetraureadioxouranium(VI) nitrate. *Inorg. Chem.* **1972**, *11*, 1840−1845. (b) Zalkin, A.; Ruben, H.; Templeton, D. H. Structure of pentakis(urea)dioxouranium(VI) nitrate, $[UO_2(OC(NH_2)_2)_5](NO_3)_2$. *Inorg. Chem.* **1979**, *18*, 519−521. (c) Harrowfield, J. M.; Kepert, D. L.; Patrick, J. M.; White, A. H.; Lincoln, S. F. Notes. Crystal structure of pentakis(dimethyl sulphoxide-O)dioxouranium(VI) bis(perchlorate). *J. Chem. Soc., Dalton Trans.* **1983**, 393−396. (d) Takao, K.; Takao, S.; Ikeda, Y.; Bernhard, G.; Hennig, C. Uranyl−halide complexation in N,N-dimethylformamide: halide coordination trend manifests hardness of $[UO_2]^{2+}$. *Dalton Trans.* **2013**, *42*, 13101−13111.

(21) (a) Kersten, B.; Hawthorne, K.; Williamson, M.; Akolkar, R.; Duval, C. E. The Future of Nuclear Energy: Electrochemical Reprocessing of Fuel Takes Center Stage. *Electrochem. Soc. Interface* **2021**, *30*, 45−49. (b) Costa Peluzo, B. M.; Kraka, E. Uranium: The Nuclear Fuel Cycle and Beyond. *Int. J. Mol. Sci.* **2022**, *23*, 4655.

(22) (a) Van Staveren, C. J.; Fenton, D. E.; Reinhoudt, D. N.; Van Eerden, J.; Harkema, S. Co-complexation of urea and UO_2^{2+} in a Schiff base macrocycle: a mimic of an enzyme binding site. *J. Am. Chem. Soc.* **1987**, *109*, 3456−3458. (b) Van Staveren, C. J.; Van Eerden, J.; Van Veggel, F. C. J. M.; Harkema, S.; Reinhoudt, D. N. Cocomplexation of neutral guests and electrophilic metal cations in synthetic macrocyclic hosts. *J. Am. Chem. Soc.* **1988**, *110*, 4994−5008.

(23) Kumar, A.; Lionetti, D.; Day, V. W.; Blakemore, J. D. Trivalent Lewis Acidic Cations Govern the Electronic Properties and Stability of Heterobimetallic Complexes of Nickel. *Chem.—Eur. J.* **2018**, *24*, 141−149.

(24) Golwankar, R. R.; Kumar, A.; Day, V. W.; Blakemore, J. D. Revealing the Influence of Diverse Secondary Metal Cations on Redox-Active Palladium Complexes. *Chem.—Eur. J.* **2022**, *28*, No. e202200344.

(25) Kelsey, S. R.; Kumar, A.; Oliver, A. G.; Day, V. W.; Blakemore, J. D. Promotion and Tuning of the Electrochemical Reduction of Hetero- and Homobimetallic Zinc Complexes. *ChemElectroChem* **2021**, *8*, 2792−2802.

(26) Dopp, C. M.; Golwankar, R. R.; Kelsey, S. R.; Douglas, J. T.; Erickson, A. N.; Oliver, A. G.; Day, C. S.; Day, V. W.; Blakemore, J. D. Vanadyl as a Spectroscopic Probe of Tunable Ligand Donor Strength in Bimetallic Complexes. *Inorg. Chem.* **2023**, *62*, 9827−9843.

(27) Dopp, C. M. Cations on Board, Ready for Takeoff: Using Vanadyl and Its Terminal Oxo to Probe Ligand Donor Strength in Heterobimetallic Complexes, Undergraduate Thesis, University of Kansas, May 2023. https://hdl.handle.net/1808/34384 (accessed Feb 17, 2024).

(28) Berthet, J. C.; Lance, M.; Nierlich, M.; Ephritikhine, M. Simple Preparations of the Anhydrous and Solvent-Free Uranyl and Cerium(IV) Triflates $UO_2(OTf)_2$ and $Ce(OTf)_4^-$ Crystal Structures of $UO_2(OTf)_2(py)_3$ and $[\{UO_2(py)_4\}_2(\mu\text{-}O)]\ [OTf]_2$. *Eur. J. Inorg. Chem.* **2000**, *2000*, 1969−1973.

(29) Golwankar, R. R.; Curry, T. D., II; Paranjothi, C. J.; Blakemore, J. D. Molecular Influences on the Quantification of Lewis Acidity with Phosphine Oxide Probes. *Inorg. Chem.* **2023**, *62*, 9765−9780.

(30) Cowie, B. E.; Purkis, J. M.; Austin, J.; Love, J. B.; Arnold, P. L. Thermal and Photochemical Reduction and Functionalization Chemistry of the Uranyl Dication, $[U^{VI}O_2]^{2+}$. *Chem. Rev.* **2019**, *119*, 10595−10637.

(31) Yang, L.; Powell, D. R.; Houser, R. P. Structural variation in copper(i) complexes with pyridylmethylamide ligands: structural analysis with a new four-coordinate geometry index, τ_4. *Dalton Trans.* **2007**, 955−964.

(32) (a) Galloy, J.; Watson, W. H.; Vogtle, F.; Mueller, W. M. A 1:2 host-guest complex formed between 1,4,7,10,13,16-hexaoxacyclooctadecane (18-crown-6) and phenyl carbamate. *Acta Crystallogr., Sect. B: Struct. Crystallogr. Cryst. Chem.* **1982**, *38*, 1245−1248. (b) De Boer, J. A. A.; Reinhoudt, D. N.; Harkema, S.; Van Hummel, G. J.; De Jong, F. Thermodynamic constants of complexes of crown ethers and uncharged molecules and x-ray structure of the 18-crown-6•$(MeNO_2)_2$ complex. *J. Am. Chem. Soc.* **1982**, *104*, 4073−4076. (c) Engel, E. R.; Smith, V. J.; Bezuidenhout, C. X.; Barbour, L. J. Uniaxial negative thermal expansion facilitated by weak host−guest interactions. *Chem. Commun.* **2014**, *50*, 4238−4241. (d) Grassl, T.; Hamberger, M.; Korber, N. Acetylene-ammonia-18-crown-6 (1/2/1). *Acta Crystallogr. E* **2012**, *68*, o2933.

(33) (a) Zanello, P.; Nervi, C.; De Biani, F. F. *Inorganic Electrochemistry: Theory, Practice and Application*; Royal Society of Chemistry, 2019; pp 55−58. (b) Savéant, J.-M. *Elements of Molecular and Biomolecular Electrochemistry*; Wiley: Hoboken, NJ, 2019; pp 2−9.

(34) Fortier, S.; Hayton, T. W. Oxo ligand functionalization in the uranyl ion (UO_2^{2+}). *Coord. Chem. Rev.* **2010**, *254*, 197−214.

(35) Connelly, N. G.; Geiger, W. E. Chemical redox agents for organometallic chemistry. *Chem. Rev.* **1996**, *96*, 877−910.

(36) (a) Schnaars, D. D.; Wu, G.; Hayton, T. W. Borane-Mediated Silylation of a Metal−Oxo Ligand. *Inorg. Chem.* **2011**, *50*, 4695−4697. (b) Pedrick, E. A.; Wu, G.; Kaltsoyannis, N.; Hayton, T. W. Reductive silylation of a uranyl dibenzoylmethanate complex: an example of controlled uranyl oxo ligand cleavage. *Chem. Sci.* **2014**, *5*, 3204−3213. (c) Bell, N. L.; Shaw, B.; Arnold, P. L.; Love, J. B. Uranyl to uranium(IV) conversion through manipulation of axial and equatorial ligands. *J. Am. Chem. Soc.* **2018**, *140* (9), 3378−3384. (d) Mizuoka, K.; Tsushima, S.; Hasegawa, M.; Hoshi, T.; Ikeda, Y. Electronic Spectra of Pure Uranyl(V) Complexes: Characteristic Absorption Bands Due to a $U^VO_2^+$ Core in Visible and Near-Infrared Regions. *Inorg. Chem.* **2005**, *44*, 6211−6218. (e) Graves, C. R.; Scott, B. L.; Morris, D. E.; Kiplinger, J. L. Facile access to pentavalent uranium organometallics: one-electron oxidation of uranium (IV) imido complexes with copper (I) salts. *J. Am. Chem. Soc.* **2007**, *129*, 11914−11915.

(37) Pantazis, D. A.; Neese, F. All-electron scalar relativistic basis sets for the actinides. *J. Chem. Theory Comput.* **2011**, *7*, 677−684.

(38) Weigend, F.; Ahlrichs, R. Balanced basis sets of split valence, triple zeta valence and quadruple zeta valence quality for H to Rn: Design and assessment of accuracy. *Phys. Chem. Chem. Phys.* **2005**, *7*, 3297−3305.

(39) Barone, V.; Cossi, M. Quantum Calculation of Molecular Energies and Energy Gradients in Solution by a Conductor Solvent Model. *J. Phys. Chem. A* **1998**, *102*, 1995−2001.

(40) Landis, C. R.; Weinhold, F. The NBO view of chemical bonding. *The Chemical Bond: Fundamental Aspects of Chemical Bonding*; Wiley-VCH, 2014; pp 91−120.

(41) Glendening, E. D.; Landis, C. R.; Weinhold, F. Natural bond orbital theory: Discovering chemistry with NBO7. *Complementary Bonding Analysis*; De Gruyter, 2021; pp 129−156.

(42) Glendening, E. D.; Badenhoop, J. K.; Reed, A. E.; Carpenter, J. E.; Bohmann, J. A.; Morales, C. M.; Karafiloglou, P.; Landis, C. R.; Weinhold, F. *NBO 7.0*; Theoretical Chemistry Institute, University of Wisconsin: Madison, WI, 2018.

https://doi.org/10.1021/jacs.3c12075
J. Am. Chem. Soc. XXXX, XXX, XXX−XXX